Altered basal forebrain regulation of intrinsic brain networks in depressive and anxiety disorders

*Alec J. Jamieson [1], Trevor Steward [1,2], Christopher G Davey [1], Sevil Ince [1,2], James A Agathos [1], Bradford A Moffat [3], Rebecca K Glarin [3], Kim L Felmingham [2], Ben J Harrison[1]

[1] Department of Psychiatry, The University of Melbourne, Parkville, Australia

[2] Melbourne School of Psychological Sciences, The University of Melbourne, Parkville, Australia

[3] The Melbourne Brain Centre Imaging Unit, Department of Radiology, The University of Melbourne, Parkville, Australia

***Corresponding author:** Dr. Alec Jamieson. Department of Psychiatry, The University of Melbourne. Level 3, 161 Barry St. Carlton, VIC 3053. Phone: (+61) 449 501 556 | Email: alec.jamieson@unimelb.edu.au

Keywords: Basal forebrain; Effective connectivity; Depressive disorders; Anxiety disorders; Resting-state

Word count: 4061

Abstract

Altered connectivity both within and between the default mode and salience networks have been observed across depressive and anxiety disorders. Recent work has highlighted the importance of subcortical regions, including subdivisions of the basal forebrain, in coordinating the activity of these networks. However, the precise influence of basal forebrain subregions on intrinsic networks across these disorders remains unknown. Using ultra-high field (7-Tesla) functional magnetic resonance imaging, we examined the resting-state effective connectivity of three basal forebrain subregions in a transdiagnostic sample of 70 individuals with mental health conditions, predominantly depressive and anxiety disorders, compared to 77 healthy controls. We explored connectivity between these subregions and regions of the salience network (anterior insula and dorsal anterior cingulate) and default mode network (ventromedial prefrontal cortex, posterior cingulate cortex, and inferior parietal lobule). Clinical participants showed increased inhibitory connectivity from the nucleus basalis of Meynert to regions of the default mode network and dorsal anterior cingulate. Increased inhibitory connectivity was also observed from the ventral pallidum to regions of the posterior default mode network. These transdiagnostic changes in the basal forebrain's regulation of large-scale cortical networks across may suggest novel mechanistic avenues for pharmacological treatments, including cholinergic system targeting.

Widespread alterations to intrinsic brain network activity have been noted across depressive and anxiety disorders [1-3]. These mental health conditions have been specifically associated with connectivity changes in the default mode (DMN) and salience networks [4,5]. Abnormal DMN connectivity in major depressive disorder (MDD) has been associated with higher levels of rumination and an increased duration of depressive episodes [6]. Similarly, altered resting-state connectivity, both within the DMN and between the DMN and salience network, has been observed across both social and generalized anxiety disorders [7] and associated with anxiety symptom severity [8]. Abnormal functioning of these networks has been hypothesized to relate to common symptoms across both conditions. For example, DMN alterations are suggested to contribute to abnormal self-referential processing and rumination, whereas dysfunction in the salience network may relate to abnormal processing of negative stimuli [9-11]. Despite the possible transdiagnostic nature of these effects, reliance on categorical diagnoses rather than symptoms, has limited investigations into the generalisability [12,13].

Although the DMN and salience networks are primarily identified as cortical in nature, there is emerging evidence that their function is heavily influenced by subcortical modulatory structures, including the basal forebrain [14-16]. The basal forebrain's influence over the DMN has been hypothesized to reflect a mechanism for switching between internally and externally directed attention states [15,17]. Activation of cholinergic neurons in the basal forebrain of rodents has been shown to decrease DMN functional connectivity, highlighting a potential role of the basal forebrain in regulating the activity of this network [18]. Notably, the cholinergic component of the basal forebrain demonstrates distinct subdivisions with heterogeneity demonstrated in both their histochemistry and function [19]. These subregions include the medial septal nucleus (cholinergic group 1; Ch1), vertical nucleus of the diagonal band (Ch2), horizontal nucleus of the diagonal band (Ch3), and nucleus basalis of Meynert (Ch4) [19]. Notably, Ch4 demonstrates the highest concentration of cholinergic cells,

comprising approximately 90% of its neurons, and represents the major source of cholinergic innervation for the cortical mantle [19]. These basal forebrain subdivisions are largely replicated in resting-state fMRI functional connectivity studies, with Fritz and colleagues illustrating two functional subcomponents congruent with Ch1-3 and Ch4 [20]. Importantly these subregions demonstrate differential connectivity patterns with intrinsic cerebral networks, with Ch1-3 exhibiting a strong functional connectivity with the anterior DMN, whereas Ch4 activity is correlated with the functioning of the salience and central executive networks [20-22]. In contrast, the ventral pallidum (VP), a basal forebrain subregion which is predominantly GABAergic [23], has also demonstrated evidence for controlling transitions between internally and externally guided behavior by regulating DMN activity [14,24,25]. This indicates that different subregions of the basal forebrain may have distinct and overlapping roles in coordinating the activity of different intrinsic brain networks.

The basal forebrain is implicated in functions that are known to be altered across depression and anxiety, including the modulation of circadian rhythms, appetite, motivation, and cognitive flexibility [26-28]. There is also consistent evidence that reductions in acetylcholinesterase activity and increasing acetylcholine levels can induce depression and anxiety symptoms in humans and rodents [29,30]. Rodent work suggests that both lesions in cholinergic neurons and stress-induced hyperactivity of VP GABAergic neurons can produce depression-like behaviors [31,32]. Importantly, these behaviors induced by cholinergic lesions appear reversable with both ketamine and fluoxetine treatment [31]. Together this indicates that basal forebrain disturbances may be present across anxiety and depressive disorders and contribute to changes observed in the functioning of intrinsic networks. However, research on the functioning of the basal forebrain and its subregions remains limited in humans due to the technical limitations of conventional (3-Tesla) fMRI approaches [33].

To address this gap, we examined the role of basal forebrain subregions, specifically Ch1-3, Ch4, and VP, in coordinating the activity of regions of the DMN and salience network using ultra high field (7-Tesla) fMRI. We used spectral dynamic causal modeling (DCM) [34,35] to examine alterations to effective connectivity (i.e., directional influences among brain regions) in a transdiagnostic sample. We hypothesized that this clinical sample would be characterized by greater influence from basal forebrain regions to the DMN, particularly from Ch1-3 and the VP due to their greater association with the DMN activity [14,20,24,25]. We additionally hypothesized that altered effective connectivity would be associated with both depression and anxiety symptom severity.

Results

Demographic and Clinical Differences

As expected, clinical participants' scores were significantly greater than healthy controls on the total DASS scale and across all three subscales (Table 2). The proportion of female clinical participants was significantly higher than in the healthy control group ($X^2 = 12.26$, $p = .003$). However, there were no significant differences in DASS total scores between male and females within the healthy control ($t(75) = .84$, $p = .201$) or clinical groups ($t(28.86) = .05$, $p = .479$). No other demographic differences were observed between the two groups (Table 1).

Effective Connectivity Differences in Clinical Participants and Healthy Controls

Overall, healthy controls demonstrated an excitatory influence from Ch1-3 over the vmPFC (0.20 Hz), PCC (0.12 Hz), left IPL (0.13 Hz) and VP (0.09 Hz) and an inhibitory influence over the anterior insula (R: -0.40 Hz; L: -0.36 Hz) and dACC (-0.14 Hz). Ch4 illustrated an excitatory influence over the anterior insula (R:0.28 Hz; L:0.26 Hz) and VP (0.17 Hz) and an

inhibitory influence over the vmPFC (-0.26 Hz), PCC (-0.54 Hz), and IPL (R: -0.55 Hz; L: -0.59 Hz). Finally, VP showed an excitatory influence over Ch1-3 (0.07 Hz), Ch4 (0.26 Hz), and the left anterior insula (0.11 Hz) and an inhibitory influence over the vmPFC (-0.20 Hz), PCC (-0.27 Hz), IPL (R: -0.40 Hz; L: -0.47 Hz).

Compared with healthy controls, clinical participants demonstrated strong evidence for greater inhibitory connectivity from Ch4 to the vmPFC (-0.30 Hz), dACC (-0.20 Hz), PCC (-0.24 Hz), and IPL (R: -0.27; L: -0.29; Figure 2A). Clinical participants also demonstrated greater excitatory connectivity from Ch4 to bilateral anterior insula (R: 0.13; Hz; L: 0.12 Hz) and from the left anterior insula to Ch4 (0.07 Hz), as well as reduced excitatory connectivity from Ch4 to VP (-0.12 Hz) and to Ch1-3 (-0.10 Hz).

Clinical participants were observed to have greater excitatory connectivity from the VP to the right anterior insula (0.21 Hz), whereas greater inhibitory connectivity was observed from the VP to the PCC (-0.14 Hz), and bilateral IPL (R: -0.27 Hz; L: -0.24 Hz). Reduced excitatory connectivity from the vmPFC (-0.06 Hz) and greater connectivity from the left anterior insula (-0.10 Hz) to the VP were also observed (Figure 2B).

Clinical participants additionally illustrated several notable effects involving Ch1-3, specifically reduced excitatory connectivity to the right IPL (-0.16 Hz) as well as reduced inhibitory connectivity to the right IPL (0.06 Hz). The vmPFC demonstrated greater self-inhibition (.13), whereas the PCC was observed to have reduced self-inhibition (-.16). See Supplementary Table S1 for a full list of connectivity parameters.

Leave-one-out Cross Validation

Given that connectivity alterations largely implicated Ch4 and VP, we then tested whether the size of the effect of group on the connectivity between these regions and cortical regions was sufficiently large to predict symptom severity. This analysis revealed that connectivity

alterations involving cortical midline regions were associated with overall negative emotional state (vmPFC/dACC: $r = 0.25$, $p < 0.05$; PCC: 0.15, $p < 0.05$), whereas connectivity involving lateralized regions such as the anterior insula ($r = -0.27$: $p = 0.99$) and IPL ($r = -0.02$, $p = 0.58$) were not. Using the altered connectivity of the vmPFC, dACC, PCC and basal forebrain regions together resulted in an overall correlation of $r = 0.31$, $p < 0.05$ (Figure 3). This overall effect did not appear to be driven any of the DASS subscales, with depressive ($r = 0.30$, $p < .05$), stress-tension ($r = 0.27$, $p < .05$), or anxiety symptoms ($r = 0.26$, $p < 0.05$) demonstrating similar correlations.

Discussion

This study examined alterations in basal forebrain resting-state effective connectivity across depressive and anxiety disorders. Our findings highlight the differential roles of Ch1-3, Ch4, and VP in coordinating intrinsic brain networks. We identified that people with depressive and anxiety disorders demonstrated altered regulation of the DMN and salience networks stemming from Ch4 and VP. Notably, altered connections between the basal forebrain and cortical midline regions were predictive of participants' negative mood state. Our results both support the basal forebrain's role in the coordination of the DMN and salience network and demonstrate that alterations in this circuitry relate to broad negative affective symptoms.

The basal forebrain contains a heterogeneous population of neurons, including GABAergic, cholinergic, glutamatergic, and peptidergic neurons [36-38], which interact locally in addition to projecting cortically [39]. Parvalbumin positive GABAergic neurons have emerged as likely candidates for the anatomical substrate of the basal forebrain responsible for DMN regulation [40,41]. These GABAergic neurons have been shown to project to major DMN nodes, including the anterior cingulate and retrosplenial cortices [42,43]. Optogenetic work has specifically identified causal evidence for the critical role of parvalbumin positive

neurons in triggering state switching by activating the DMN and inducing associated behaviors [42]. These effects are also consistent with observations from VP GABAergic neurons, with stimulation of these neurons being shown to automatize internally focused behavior and impair attention directed towards external stimuli [25]. This function mirrors increased ruminative thought observed across depressive and anxiety disorders [44]. Moreover, local optogenetic inhibition of VP GABAergic neurons triggers transitions from quiet wakefulness to exploratory behavior, with associated cortical activation being partially dependent on cholinergic transmission [45]. Acetylcholine release and activity from cholinergic neurons in the basal forebrain have also been shown to be associated with reductions in DMN activity and connectivity [18,46]. Together this indicates that regulation of the DMN likely occurs through both cholinergic and non-cholinergic mechanisms within the basal forebrain, consistent with findings from our current study.

Previous research has reported greater negative connectivity from the anterior DMN to regions of the salience and central executive networks in MDD [9], indicating an increased influence of the DMN on these other networks [47]. These effects are congruent with research identifying that MDD is characterized by greater time spent in a coactivation pattern involving both activation of the DMN and deactivation of the frontoparietal network [48]. This DMN dominance has been hypothesized to underlie a dysfunctional ability to shift attention from self-directed thoughts to external, goal-related behavior in MDD [49,50]. Notably, the results of the current study and others indicate that these effects are directly influenced by changes in basal forebrain activity [14,16,25]. The fact that the largest effects were observed in regards to Ch4 connectivity is notable given its high proportion of cholinergic neurons [19]. The cholinergic basal forebrain system has been hypothesized to modulate information processing and attention by enhancing functional segregation within the brain [51]. This is further corroborated by more recent research which has shown that local inactivation of Ch4 leads to

a decrease in the energy barriers required for a state transition in cortical activity, thereby increasing the likelihood of transitioning between different brain states [52,53]. Dysfunction of the cholinergic system has been implicated in the development of cognitive impairments consistent with depression and anxiety symptoms, including attentional deficits, memory dysfunction, and negativity biases [54,55]. This association with negativity bias may, in part, explain the relationship between Ch4 circuitry dysfunction and broad negative mood symptoms highlighted above. As such, a combination of abnormal influences from both the VP and Ch4 may result in altered DMN activity and an impaired ability to switch between network states [14], which in turn contributes to the development of depression and anxiety symptoms.

Dysfunctional Ch4 connectivity across these disorders may have direct implications for treatment using medications that affect cholinergic transmission. Scopolamine is a nonspecific muscarinic receptor antagonist which has demonstrated some evidence as a rapid antidepressant and anxiolytic, with effects occurring as quickly as 3 days post-infusion [56-58]. However, there have been relatively few high-quality trials investigating scopolamine's antidepressant effects and these studies have demonstrated inconsistent evidence for its effectiveness due to differences in administration routes and dosage [57,59]. This observed variability in response may also be indicative of a specific underlying biotype which demonstrates sensitivity to this treatment. Relatively few investigations have been undertaken to identify potential predictors of improved treatment response to scopolamine [60]. However, growing evidence indicates that scopolamine's rapid antidepressant effects, akin to other rapid antidepressant such as ketamine, occurs via inhibition of GABAergic interneurons in the mPFC [61]. Given the highlighted role of the basal forebrain in coordinating the activity of the DMN and changes in this circuitry in depressive and anxiety disorders, investigation into

the utility of these connectivity alterations in predicting response to scopolamine is warranted.

Limitations

While the transdiagnostic nature of the clinical group under investigation is a strength of the study and is representative of community samples, using discrete diagnostic categories to investigate this circuitry and its relationship with specific symptoms may be more useful in identifying specific clinical targets. Notably, 15 participants were excluded from our analysis due in insufficient mapping of BOLD signal in one or more of the regions, which was largely driven by signal dropout in basal forebrain subregions and potentially introduces a risk of selection bias. While 7T fMRI has many advantages over 3T, it also has several notable drawbacks including increased susceptibility artifacts which may have contributed to this issue [62]. Given the role of the cholinergic system in modulating arousal and attention [63], physiological measure such as eye tracking may have provided greater insight into the discrete time periods in which this circuitry was most active and as such should be integrated into future research. Using structural connectivity priors to constrain the inversion of resting-state effective connectivity have been shown to increase model evidence for most intrinsic networks, and thus may enhance the translational utility of these parameters by enhancing both test-retest reliability and out-of-sample validity [64].

Conclusions

To our knowledge, this is the first study to examine alterations in basal forebrain subregion effective connectivity in people with depressive and anxiety disorders. This work supports the notion that the basal forebrain is an important functional regulator of intrinsic brain networks and that different subregions have unique relationships with these networks. We identified

widespread increased inhibition from Ch4 to regions of the DMN and the dACC. Similar alterations were observed from the VP to regions of the posterior DMN. Dysfunction between these basal forebrain subregions and cortical midline regions were observed to be predictive of non-specific negative mood states. While a putative cholinergic basis of the aforementioned dysfunction needs to be established through future research, this may have implications for novel treatment targeting in depressive and anxiety disorders.

Methods

A transdiagnostic sample of 79 clinical participants were recruited to the study from The University of Melbourne Psychology Clinic and via the Research Experience Program at the Melbourne School of Psychological Sciences. All clinical participants underwent the Diagnostic Interview for Anxiety, Mood, and OCD and Related Neuropsychiatric Disorders (DIAMOND) [65], a semi-structured clinical interview based on DSM-5 diagnostic criteria, to identify those who met criteria for a mood and/or anxiety disorder. Participants were also included if they met criteria for stress and/or eating disorders due to the high level of depressive and anxiety symptoms present in these conditions [66,67]. Participants who met criteria for psychosis, bipolar disorder, paraphilic disorder, dissociative disorder, or conduct disorder were excluded. Clinical participants were compared to 92 matched control participants recruited via publicly accessible online advertisements. These participants had no current or past diagnosis of a mental health disorder as assessed through the Mini-International Neuropsychiatric Interview-7 [68]. All participants were between 18 to 40 years of age, fluent English speakers, had no MRI contraindications including pregnancy, and had normal or corrected-to-normal visual acuity. All participants provided written informed consent prior to the study, following a complete description of the study protocol. This study and its protocol were approved by the Melbourne Health Human Research and Ethics

Committee. All participants attended a single 7T scanning session at the Melbourne Brain Imaging Unit (The University of Melbourne, Parkville). The Depression, Anxiety and Stress Scale short-form (DASS-21) was administered prior to the session to provide an overall measure of negative mood states, as well as sub-scales scores of depression, anxiety, and stress-tension [69]. Of the original sample, three participants were excluded due to data quality issues (three controls), five participants were excluded due to excessive head movement during scanning (four controls and one clinical participant), and 16 due to insufficient activity mapping across all regions necessary for DCM (11 controls and five clinical participants; for further details see Times Series Extraction below). This resulted in 70 clinical participants and 77 healthy controls being included in the primary analysis.

Image Acquisition

MRI acquisition was performed on a Siemens 7T Plus research scanner (Siemens Healthcare, Erlangen, Germany) equipped with a 32Rx/1Tx channel head coil (Nova Medical Inc., Wilmington MA, USA). Functional (T2*-weighted) images were obtained using a multi-band and grappa accelerated gradient-echo planar imaging (GE-EPI) sequence [70] in the steady state (multi-band factor, 6; parallel acceleration factor, 2; repetition time, 800 ms; echo time, 22.2 ms; flip angle, 45°) in a 20.8 cm field-of-view, with a 130×130-pixel matrix, a slice thickness of 1.6mm (no gap) and in-plane voxel size=1.6×1.6 mm. Eighty-four interleaved slices were acquired parallel to the anterior-posterior commissure line, covering the whole brain. The resting-state sequence duration was 5 minutes and 20 seconds, corresponding to 400 whole-brain echo-planar imaging volumes. Participants were instructed to keep their eyes closed but not to fall asleep for the duration of the scan.

A high resolution structural T1-weighted image was obtained from each participant using magnetization-prepared 2 rapid gradient echo sequence (MP2RAGE [71]) for co-

registration with the functional images (parallel reduction factor, 4; repetition time, 5 seconds; echo time, 2.04 ms; flip angle, 13°) in a 24 cm field of view, with a 330×330–pixel matrix, in-plane voxel size = 0.75×0.75 mm, slice thickness = 0.75 mm with 224 sagittal slices aligned parallel to the midline. To minimize head movement during scanning, foam pads were inserted to the either side of participants' heads. Respiration and cardiac pulse were also recorded during the session at 200 hertz (Hz) and 50 Hz, respectively, using a respiratory belt and pulse-oximeter (Siemens, Germany) to be used for physiological noise correction.

Preprocessing

Imaging data were preprocessed using Statistical Parametric Mapping (SPM) 12 (v7771, Welcome Trust Centre for Neuroimaging, London, UK) within a MATLAB 2023b environment (The MathWorks Inc., Natick, MA) on Spartan High Performance Computer hosted at The University of Melbourne [72]. Motion artifacts were corrected by realigning each participant's timeseries to the mean image, and all images were resampled using 4th Degree B-Spline interpolation. Participants were excluded if movement exceeded a mean total displacement of 1.6mm (~1 native voxel) as assessed through the Motion Fingerprint toolbox [73].

Each participant's anatomical images (denoised MP2RAGE [74]) were co-registered to their respective mean functional image, segmented, and normalized to the International Consortium of Brain Mapping template using the unified segmentation and the Diffeomorphic Anatomical Registration Through Exponentiated Lie Algebra approach [75]. Smoothing was applied with a 3.2-mm^3 full-width-at-half-maximum Gaussian kernel to preserve spatial specificity. Physiological noise was modeled using PhysIO toolbox [76]. Cardiac and respiratory recordings were imported to the toolbox, in which physiological noise models were applied to these recordings (i.e., the retrospective image-based correction

for a third order cardiac, fourth order respiratory, and first order interaction Fourier expansion of cardiac and respiratory phase [77]; respiratory volume per time [78]; heart rate variability response [79]). Normalized white matter and cerebrospinal fluid tissue segmentations from each participant's structural image were used to construct noise regions of interest from which mean timeseries and principal components were extracted as nuisance regressors using CompCor [80]. These regressors were added to six movement regressors estimated through realignment and taken to the first-level general linear model to remove variances of no-interest.

Spectral Dynamic Causal Modeling

DCM is a technique used to infer directional influences among brain regions, or effective connectivity, based on functional neuroimaging data [81,82]. While traditional deterministic and stochastic DCM operates by analyzing the timeseries data directly, spectral DCM estimates effective connectivity using the cross-spectral density (for further details see Supplementary Methods). This is a second-order summary statistic of the timeseries data and thus allows the estimation of effective connectivity parameters for resting-state data with a greatly increased computational efficiency [83]. Effective connectivity between regions is measured in Hz, with positive values being indicative of putative excitation between regions while negative values represent putative inhibition. Self or within-region connections are represented by unitless log scaling parameters that modify the default inhibitory connectivity of -0.5Hz. As such, positive values for these parameters are indicative of greater inhibition whereas negative values represent reduced inhibition.

Timeseries Extraction and Model Specification

The Montreal Neurological Institute coordinates for core regions of the DMN and salience network were identified using previously reported peak coordinates from meta-analyses and large-scale functional connectivity studies. The precise coordinates were as follows: vmPFC [3, 39, -2] [84], PCC [2 -43 24] [84], IPL [44 -65 32; -40 -66 32] [85], anterior insula [36, 16, 4; -35, 14, 5] [86], dorsal anterior cingulate (dACC) [4, 30, 30] [87]. The timeseries from these VOIs were extracted using the principal eigenvariate of all voxels in a sphere within a radius of 6 mm of the centroids for midline regions (vmPFC, PCC, dACC) and 4 mm for lateralized regions (IPL and anterior insula; Supplementary Figure S1). To extract the basal forebrain subregions, we used basal forebrain masks based on the stereotaxic probabilistic maps of the magnocellular basal forebrain space by Zaborszky and colleagues [88] for Ch1-3 and 4, and the subcortical mask from Pauli and colleagues [89] for the VP (Figure 1). Seed-to-whole brain functional connectivity analyses were conducted to ensure that these masks accurately captured the intended regions and their associated functional connectivity patterns (Supplementary Methods and Results).

Our model space was specified using DCM 12.5. To address our hypotheses concerning the distinct effects of basal forebrain subregions, we modeled bidirectional connectivity to and from these subregions to all cortical regions highlighted above. Using the *spm_dcm_fmri_check* function, we assessed the explained variance of the model. This revealed an average explained variance of 86.9% across all subjects, indicating that the specified model was capturing a large degree of the observed changes in BOLD signal over time.

Parametric Empirical Bayes

To examine the impact of group differences on individual parameters, we employed Parametric Empirical Bayes (PEB) [90]. Unlike comparisons using classical frequentist tests

which only use estimated mean values, PEB allows for the inclusion of estimated variance (in addition to the estimated means) of each parameter when investigating between-group effects. The posterior probability (PP) was calculated using the free energy (with vs. without) option. This approach compares the evidence for all models in which a particular parameter is switched on with the evidence for models in which it is switched off. A PP threshold of greater than 0.99 was used to identify those parameters which had a *very strong* amount of evidence [91]. We constructed a second level PEB model including four regressors. The first regressor modeled the average connectivity observed across healthy control participants, with subsequent regressors either increasing or decreasing this baseline connectivity. The subsequent regressors included the difference between clinical participants and healthy controls, as well as age and gender as covariates. Having estimated a group level PEB model, we then searched over nested PEB models using Bayesian model reduction pruning parameters that did not contribute to overall model evidence [82,92]. Bayesian model averaging was performed on these models after the final iteration to determine the strength of connections in the last Occam's window of 256 models.

Leave-one-out Cross-validation

To assess the predictive validity of parameters which demonstrated between-group differences, we used leave-one-out cross-validation (LOOCV) across all participants. In the PEB framework, LOOCV aims to determine whether the size of between-group effects on parameters is sufficiently large to predict a variable of interest [91]. In this case, this was employed to determine whether identified parameters were related to symptom severity. A group-level PEB model was estimated for all participants while excluding one participant, then this PEB model was used to predict the left-out subject's DASS scores. These predicted scores were then correlated with the observed symptom severity. A significant correlation

between the expected and observed values demonstrates that the effect size was sufficiently large to predict the left-out subjects' symptom severity above chance (see [91] for further details).

Declaration of Competing and Financial Interests

The authors declare no biomedical financial interests or potential conflicts of interest.

Funding

This study was supported by National Health and Medical Research Council of Australia (NHMRC) Project Grants (1161897) to BJH and (1073041) to KLF. TS is supported by a NHMRC/MRFF Investigator Grant (MRF1193736), a BBRF Young Investigator Grant, and a University of Melbourne McKenzie Fellowship. JA and SI are supported by Australian Government Research Training Program Scholarships.

Acknowledgements

The authors thank Braden Thai, Holly Carey and Amy Nielson for their contributions to data collection. The authors also acknowledge the facilities and scientific and technical assistance of the National Imaging Facility, a National Collaborative Research Infrastructure Strategy (NCRIS) capability, at the Melbourne Brain Centre Imaging Unit, University of Melbourne. In addition, the authors are grateful to Siemens for providing the MP2RAGE sequence as a “works in progress package” and CMRR (University of Minnesota) for sharing the multiband EPI sequence.

References

1 Dutta, A., McKie, S. & Deakin, J. F. Resting state networks in major depressive disorder. *Psychiatry Res* **224**, 139-151 (2014). https://doi.org/10.1016/j.pscychresns.2014.10.003

2 Bertocci, M. A. *et al.* Altered patterns of central executive, default mode and salience network activity and connectivity are associated with current and future depression risk in two independent young adult samples. *Mol Psychiatry* **28**, 1046-1056 (2023). https://doi.org/10.1038/s41380-022-01899-8

3 Zhang, X. *et al.* Large-scale brain functional network abnormalities in social anxiety disorder. *Psychol Med* **53**, 6194-6204 (2023). https://doi.org/10.1017/S0033291722003439

4 Mulders, P. C., van Eijndhoven, P. F., Schene, A. H., Beckmann, C. F. & Tendolkar, I. Resting-state functional connectivity in major depressive disorder: A review. *Neurosci Biobehav Rev* **56**, 330-344 (2015). https://doi.org/10.1016/j.neubiorev.2015.07.014

5 Tse, N. Y. *et al.* A mega-analysis of functional connectivity and network abnormalities in youth depression. *Nature Mental Health* **2**, 1169-1182 (2024). https://doi.org/10.1038/s44220-024-00309-y

6 Mohan, A. *et al.* The Significance of the Default Mode Network (DMN) in Neurological and Neuropsychiatric Disorders: A Review. *Yale J Biol Med* **89**, 49-57 (2016).

7 Rabany, L. *et al.* Resting-State Functional Connectivity in Generalized Anxiety Disorder and Social Anxiety Disorder: Evidence for a Dimensional Approach. *Brain Connect* **7**, 289-298 (2017). https://doi.org/10.1089/brain.2017.0497

8 Li, R. *et al.* Dissociable salience and default mode network modulation in generalized anxiety disorder: a connectome-wide association study. *Cereb Cortex* **33**, 6354-6365 (2023). https://doi.org/10.1093/cercor/bhac509

9 Jamieson, A. J., Harrison, B. J., Razi, A. & Davey, C. G. Rostral anterior cingulate network effective connectivity in depressed adolescents and associations with treatment response in a randomized controlled trial. *Neuropsychopharmacology* **47**, 1240-1248 (2022). https://doi.org/10.1038/s41386-021-01214-z

10 Jamieson, A. J. *et al.* A brain model of altered self-appraisal in social anxiety disorder. *Transl Psychiatry* **13**, 344 (2023). https://doi.org/10.1038/s41398-023-02644-7

11 Xu, L., Xu, H., Ding, H., Li, J. & Wang, C. Intrinsic Network Brain Dysfunction Correlates With Temporal Complexity in Generalized Anxiety Disorder and Panic Disorder. *Front Hum Neurosci* **15**, 647518 (2021). https://doi.org/10.3389/fnhum.2021.647518

12 Deif, R. & Salama, M. Depression From a Precision Mental Health Perspective: Utilizing Personalized Conceptualizations to Guide Personalized Treatments. *Front Psychiatry* **12**, 650318 (2021). https://doi.org/10.3389/fpsyt.2021.650318

13 Dalgleish, T., Black, M., Johnston, D. & Bevan, A. Transdiagnostic approaches to mental health problems: Current status and future directions. *J Consult Clin Psychol* **88**, 179-195 (2020). https://doi.org/10.1037/ccp0000482

14 Aguilar, D. D. & McNally, J. M. Subcortical control of the default mode network: Role of the basal forebrain and implications for neuropsychiatric disorders. *Brain Res Bull* **185**, 129-139 (2022). https://doi.org/10.1016/j.brainresbull.2022.05.005

15 Nair, J. *et al.* Basal forebrain contributes to default mode network regulation. *Proc Natl Acad Sci U S A* **115**, 1352-1357 (2018). https://doi.org/10.1073/pnas.1712431115

16 Alves, P. N. *et al.* An improved neuroanatomical model of the default-mode network reconciles previous neuroimaging and neuropathological findings. *Commun Biol* **2**, 370 (2019). https://doi.org/10.1038/s42003-019-0611-3

17 Harrison, B. J. *et al.* Dynamic subcortical modulators of human default mode network function. *Cereb Cortex* **32**, 4345-4355 (2022). https://doi.org/10.1093/cercor/bhab487

18 Peeters, L. M. *et al.* Cholinergic Modulation of the Default Mode Like Network in Rats. *iScience* **23**, 101455 (2020). https://doi.org/10.1016/j.isci.2020.101455

19 Mesulam, M. M., Mufson, E. J., Levey, A. I. & Wainer, B. H. Cholinergic innervation of cortex by the basal forebrain: cytochemistry and cortical connections of the septal area, diagonal band nuclei, nucleus basalis (substantia innominata), and hypothalamus in the rhesus monkey. *J Comp Neurol* **214**, 170-197 (1983). https://doi.org/10.1002/cne.902140206

20 Fritz, H. C. J. *et al.* The corticotopic organization of the human basal forebrain as revealed by regionally selective functional connectivity profiles. *Human Brain Mapping* **40**, 868-878 (2019). https://doi.org/10.1002/hbm.24417

21 Yuan, R., Biswal, B. B. & Zaborszky, L. Functional Subdivisions of Magnocellular Cell Groups in Human Basal Forebrain: Test-Retest Resting-State Study at Ultra-high Field, and Meta-analysis. *Cereb Cortex* **29**, 2844-2858 (2019). https://doi.org/10.1093/cercor/bhy150

22 Li, C. S. *et al.* Resting state functional connectivity of the basal nucleus of Meynert in humans: in comparison to the ventral striatum and the effects of age. *Neuroimage* **97**, 321-332 (2014). https://doi.org/10.1016/j.neuroimage.2014.04.019

23 Root, D. H., Melendez, R. I., Zaborszky, L. & Napier, T. C. The ventral pallidum: Subregion-specific functional anatomy and roles in motivated behaviors. *Prog Neurobiol* **130**, 29-70 (2015). https://doi.org/10.1016/j.pneurobio.2015.03.005

24 Zhao, Y., Kirschenhofer, T., Harvey, M. & Rainer, G. Mediodorsal thalamus and ventral pallidum contribute to subcortical regulation of the default mode network. *Commun Biol* **7**, 891 (2024). https://doi.org/10.1038/s42003-024-06531-9

25 Klaassen, A.-L., Heiniger, A., Sánchez, P. V., Harvey, M. A. & Rainer, G. Ventral pallidum regulates the default mode network, controlling transitions between internally and externally guided behavior. *Proceedings of the National Academy of Sciences of the United States of America* **118**, 1-10 (2021).

26 Yamakawa, G. R. *et al.* The cholinergic forebrain arousal system acts directly on the circadian pacemaker. *Proc Natl Acad Sci U S A* **113**, 13498-13503 (2016). https://doi.org/10.1073/pnas.1610342113

27 Cabrera, S. M., Chavez, C. M., Corley, S. R., Kitto, M. R. & Butt, A. E. Selective lesions of the nucleus basalis magnocellularis impair cognitive flexibility. *Behav Neurosci* **120**, 298-306 (2006). https://doi.org/10.1037/0735-7044.120.2.298

28 Herman, A. M. *et al.* A cholinergic basal forebrain feeding circuit modulates appetite suppression. *Nature* **538**, 253-256 (2016). https://doi.org/10.1038/nature19789

29 Dulawa, S. C. & Janowsky, D. S. Cholinergic regulation of mood: from basic and clinical studies to emerging therapeutics. *Mol Psychiatry* **24**, 694-709 (2019). https://doi.org/10.1038/s41380-018-0219-x

30 Mineur, Y. S. *et al.* Cholinergic signaling in the hippocampus regulates social stress resilience and anxiety- and depression-like behavior. *Proceedings of the National Academy of Sciences of the United States of America* **110**, 3573-3578 (2013).

31 Chen, L. *et al.* Fluoxetine and Ketamine Reverse the Depressive but Not Anxiety Behavior Induced by Lesion of Cholinergic Neurons in the Horizontal Limb of the Diagonal Band of Broca in Male Rat. *Front Behav Neurosci* **15**, 602708 (2021). https://doi.org/10.3389/fnbeh.2021.602708

32 Knowland, D. *et al.* Distinct Ventral Pallidal Neural Populations Mediate Separate Symptoms of Depression. *Cell* **170**, 284-297 e218 (2017). https://doi.org/10.1016/j.cell.2017.06.015

33 Keuken, M. C., Isaacs, B. R., Trampel, R., van der Zwaag, W. & Forstmann, B. U. Visualizing the Human Subcortex Using Ultra-high Field Magnetic Resonance Imaging. *Brain Topogr* **31**, 513-545 (2018). https://doi.org/10.1007/s10548-018-0638-7

34 Razi, A., Kahan, J., Rees, G. & Friston, K. J. Construct validation of a DCM for resting state fMRI. *Neuroimage* **106**, 1-14 (2015). https://doi.org/10.1016/j.neuroimage.2014.11.027

35 Friston, K. J., Kahan, J., Biswal, B. & Razi, A. A DCM for resting state fMRI. *Neuroimage* **94**, 396-407 (2014). https://doi.org/10.1016/j.neuroimage.2013.12.009

36 Zaborszky, L., Carlsen, J., Brashear, H. R. & Heimer, L. Cholinergic and GABAergic afferents to the olfactory bulb in the rat with special emphasis on the projection neurons in the nucleus of the horizontal limb of the diagonal band. *J Comp Neurol* **243**, 488-509 (1986). https://doi.org/10.1002/cne.902430405

37 Walker, L. C. *et al.* Peptidergic neurons in the basal forebrain magnocellular complex of the rhesus monkey. *J Comp Neurol* **280**, 272-282 (1989). https://doi.org/10.1002/cne.902800208

38 Zaborszky, L., Pang, K., Somogyi, J., Nadasdy, Z. & Kallo, I. The basal forebrain corticopetal system revisited. *Ann N Y Acad Sci* **877**, 339-367 (1999). https://doi.org/10.1111/j.1749-6632.1999.tb09276.x

39 Zaborszky, L. & Duque, A. Local synaptic connections of basal forebrain neurons. *Behavioural Brain Research* **115**, 143-158 (2000). https://doi.org/https://doi.org/10.1016/S0166-4328(00)00255-2

40 Zou, Y. *et al.* Cell-type-specific optogenetic fMRI on basal forebrain reveals functional network basis of behavioral preference. *Neuron* (2024). https://doi.org/10.1016/j.neuron.2024.01.017

41 Kim, T. *et al.* Cortically projecting basal forebrain parvalbumin neurons regulate cortical gamma band oscillations. *Proc Natl Acad Sci U S A* **112**, 3535-3540 (2015). https://doi.org/10.1073/pnas.1413625112

42 Lozano-Montes, L. *et al.* Optogenetic Stimulation of Basal Forebrain Parvalbumin Neurons Activates the Default Mode Network and Associated Behaviors. *Cell Rep* **33**, 108359 (2020). https://doi.org/10.1016/j.celrep.2020.108359

43 Do, J. P. *et al.* Cell type-specific long-range connections of basal forebrain circuit. *Elife* **5** (2016). https://doi.org/10.7554/eLife.13214

44 McLaughlin, K. A. & Nolen-Hoeksema, S. Rumination as a transdiagnostic factor in depression and anxiety. *Behav Res Ther* **49**, 186-193 (2011). https://doi.org/10.1016/j.brat.2010.12.006

45 Espinosa, N. *et al.* Basal Forebrain Gating by Somatostatin Neurons Drives Prefrontal Cortical Activity. *Cereb Cortex* **29**, 42-53 (2019). https://doi.org/10.1093/cercor/bhx302

46 Sanda, P. *et al.* Cholinergic modulation supports dynamic switching of resting state networks through selective DMN suppression. *PLoS Comput Biol* **20**, e1012099 (2024). https://doi.org/10.1371/journal.pcbi.1012099

47 Liu, C. *et al.* Trait- and state-like co-activation pattern dynamics in current and remitted major depressive disorder. *J Affect Disord* **337**, 159-168 (2023). https://doi.org/10.1016/j.jad.2023.05.074

48 Dong, D. *et al.* Sex-specific resting state brain network dynamics in patients with major depressive disorder. *Neuropsychopharmacology* **49**, 806-813 (2024). https://doi.org/10.1038/s41386-024-01799-1

49 Wang, X., Ongur, D., Auerbach, R. P. & Yao, S. Q. Cognitive Vulnerability to Major Depression: View from the Intrinsic Network and Cross-network Interactions. *Harvard Rev Psychiat* **24**, 188-201 (2016). https://doi.org/10.1097/Hrp.0000000000000081

50 Berman, M. G. *et al.* Neural and behavioral effects of interference resolution in depression and rumination. *Cogn Affect Behav Ne* **11**, 85-96 (2011). https://doi.org/10.3758/s13415-010-0014-x

51 Shine, J. M. Neuromodulatory Influences on Integration and Segregation in the Brain. *Trends Cogn Sci* **23**, 572-583 (2019). https://doi.org/10.1016/j.tics.2019.04.002

52 Taylor, N. L. *et al.* Causal evidence for cholinergic stabilization of attractor landscape dynamics. *Cell Rep* **43**, 114359 (2024). https://doi.org/10.1016/j.celrep.2024.114359

53 Munn, B. R., Muller, E. J., Wainstein, G. & Shine, J. M. The ascending arousal system shapes neural dynamics to mediate awareness of cognitive states. *Nat Commun* **12**, 6016 (2021). https://doi.org/10.1038/s41467-021-26268-x

54 Shackman, A. J. *et al.* The neurobiology of dispositional negativity and attentional biases to threat: Implications for understanding anxiety disorders in adults and youth. *J Exp Psychopathol* **7**, 311-342 (2016). https://doi.org/10.5127/jep.054015

55 Dagyte, G., Den Boer, J. A. & Trentani, A. The cholinergic system and depression. *Behav Brain Res* **221**, 574-582 (2011). https://doi.org/10.1016/j.bbr.2010.02.023

56 Jaffe, R. J., Novakovic, V. & Peselow, E. D. Scopolamine as an Antidepressant: A Systematic Review. *Clin Neuropharmacol* **36**, 24-26 (2013). https://doi.org/10.1097/WNF.0b013e318278b703

57 Furey, M. L. & Drevets, W. C. Antidepressant efficacy of the antimuscarinic drug scopolamine: a randomized, placebo-controlled clinical trial. *Arch Gen Psychiatry* **63**, 1121-1129 (2006). https://doi.org/10.1001/archpsyc.63.10.1121

58 Furey, M. L., Khanna, A., Hoffman, E. M. & Drevets, W. C. Scopolamine produces larger antidepressant and antianxiety effects in women than in men. *Neuropsychopharmacology* **35**, 2479-2488 (2010). https://doi.org/10.1038/npp.2010.131

59 Mocko, P., Sladowska, K., Kawalec, P., Babii, Y. & Pilc, A. The Potential of Scopolamine as an Antidepressant in Major Depressive Disorder: A Systematic Review of Randomized Controlled Trials. *Biomedicines* **11** (2023). https://doi.org/ARTN 2636 10.3390/biomedicines11102636

60 Drevets, W. C., Bhattacharya, A. & Furey, M. L. in *Advances in Pharmacology* Vol. 89 (eds Ronald S. Duman & John H. Krystal) 357-386 (Academic Press, 2020).

61 Fogaça, M. V. *et al.* Inhibition of GABA interneurons in the mPFC is sufficient and necessary for rapid antidepressant responses. *Mol Psychiatry* **26**, 3277-3291 (2021). https://doi.org/10.1038/s41380-020-00916-y

62 Beisteiner, R. *et al.* Clinical fMRI: evidence for a 7T benefit over 3T. *Neuroimage* **57**, 1015-1021 (2011). https://doi.org/10.1016/j.neuroimage.2011.05.010

63 Larsen, R. S. & Waters, J. Neuromodulatory Correlates of Pupil Dilation. *Front Neural Circuits* **12**, 21 (2018). https://doi.org/10.3389/fncir.2018.00021

64 Greaves, M. D., Novelli, L. & Razi, A. Structurally informed resting-state effective connectivity recapitulates cortical hierarchy. *bioRxiv* (2024). https://doi.org/10.1101/2024.04.03.587831

65 Tolin, D. *et al.* Diagnostic Interview for anxiety, mood, and OCD and related neuropsychiatric disorders (DIAMOND). *Hartford, CT: The Institute of Living, Hartford Healthcare Corporation* (2016).

66 Swinbourne, J. *et al.* The comorbidity between eating disorders and anxiety disorders: prevalence in an eating disorder sample and anxiety disorder sample. *Aust N Z J Psychiatry* **46**, 118-131 (2012). https://doi.org/10.1177/0004867411432071

67 Spinhoven, P., Penninx, B. W., van Hemert, A. M., de Rooij, M. & Elzinga, B. M. Comorbidity of PTSD in anxiety and depressive disorders: prevalence and shared risk factors. *Child Abuse Negl* **38**, 1320-1330 (2014). https://doi.org/10.1016/j.chiabu.2014.01.017

68 Sheehan, D. V. *et al.* The Mini-International Neuropsychiatric Interview (MINI): the development and validation of a structured diagnostic psychiatric interview for DSM-IV and ICD-10. *J Clin Psychiat* **59**, 22-33 (1998).

69 Lovibond, S. H. Manual for the depression anxiety stress scales. *Sydney psychology foundation* (1995).

70 Moeller, S. *et al.* Multiband multislice GE-EPI at 7 tesla, with 16-fold acceleration using partial parallel imaging with application to high spatial and temporal whole-brain fMRI. *Magn Reson Med* **63**, 1144-1153 (2010). https://doi.org/10.1002/mrm.22361

71 Marques, J. P. *et al.* MP2RAGE, a self bias-field corrected sequence for improved segmentation and T1-mapping at high field. *Neuroimage* **49**, 1271-1281 (2010). https://doi.org/10.1016/j.neuroimage.2009.10.002

72 Lafayette, L., Sauter, G., Vu, L. & Meade, B. in *OpenStack Summit*.

73 Wilke, M. An alternative approach towards assessing and accounting for individual motion in fMRI timeseries. *Neuroimage* **59**, 2062-2072 (2012). https://doi.org/10.1016/j.neuroimage.2011.10.043

74 O'Brien, K. R. *et al.* Robust T1-weighted structural brain imaging and morphometry at 7T using MP2RAGE. *PLoS One* **9**, e99676 (2014). https://doi.org/10.1371/journal.pone.0099676

75 Ashburner, J. A fast diffeomorphic image registration algorithm. *Neuroimage* **38**, 95-113 (2007). https://doi.org/10.1016/j.neuroimage.2007.07.007

76 Kasper, L. *et al.* The PhysIO Toolbox for Modeling Physiological Noise in fMRI Data. *J Neurosci Meth* **276**, 56-72 (2017). https://doi.org/10.1016/j.jneumeth.2016.10.019

77 Glover, G. H., Li, T. Q. & Ress, D. Image-based method for retrospective correction of physiological motion effects in fMRI: RETROICOR. *Magn Reson Med* **44**, 162-167 (2000). https://doi.org/10.1002/1522-2594(200007)44:1<162::aid-mrm23>3.0.co;2-e

78 Birn, R. M., Smith, M. A., Jones, T. B. & Bandettini, P. A. The respiration response function: the temporal dynamics of fMRI signal fluctuations related to changes in respiration. *Neuroimage* **40**, 644-654 (2008). https://doi.org/10.1016/j.neuroimage.2007.11.059

79 Chang, C., Cunningham, J. P. & Glover, G. H. Influence of heart rate on the BOLD signal: the cardiac response function. *Neuroimage* **44**, 857-869 (2009). https://doi.org/10.1016/j.neuroimage.2008.09.029

80 Behzadi, Y., Restom, K., Liau, J. & Liu, T. T. A component based noise correction method (CompCor) for BOLD and perfusion based fMRI. *Neuroimage* **37**, 90-101 (2007). https://doi.org/10.1016/j.neuroimage.2007.04.042

81 Friston, K. J., Harrison, L. & Penny, W. Dynamic causal modelling. *Neuroimage* **19**, 1273-1302 (2003). https://doi.org/10.1016/s1053-8119(03)00202-7

82 Friston, K. J. & Penny, W. Post hoc Bayesian model selection. *Neuroimage* **56**, 2089-2099 (2011). https://doi.org/10.1016/j.neuroimage.2011.03.062

83 Novelli, L., Friston, K. & Razi, A. Spectral dynamic causal modeling: A didactic introduction and its relationship with functional connectivity. *Netw Neurosci* **8**, 178-202 (2024). https://doi.org/10.1162/netn_a_00348

84 Fair, D. A. *et al.* Functional Brain Networks Develop from a "Local to Distributed" Organization. *Plos Computational Biology* **5** (2009). https://doi.org/ARTN e1000381 10.1371/journal.pcbi.1000381

85 Yarkoni, T., Poldrack, R. A., Nichols, T. E., Van Essen, D. C. & Wager, T. D. Large-scale automated synthesis of human functional neuroimaging data. *Nat Methods* **8**, 665-670 (2011). https://doi.org/10.1038/nmeth.1635

86 Dosenbach, N. U. *et al.* Distinct brain networks for adaptive and stable task control in humans. *Proc Natl Acad Sci U S A* **104**, 11073-11078 (2007). https://doi.org/10.1073/pnas.0704320104

87 Sridharan, D., Levitin, D. J. & Menon, V. A critical role for the right fronto-insular cortex in switching between central-executive and default-mode networks. *Proceedings of the National Academy of Sciences of the United States of America* **105**, 12569-12574 (2008). https://doi.org/10.1073/pnas.0800005105

88 Zaborszky, L. *et al.* Stereotaxic probabilistic maps of the magnocellular cell groups in human basal forebrain. *Neuroimage* **42**, 1127-1141 (2008). https://doi.org/10.1016/j.neuroimage.2008.05.055

89 Pauli, W. M., Nili, A. N. & Tyszka, J. M. A high-resolution probabilistic in vivo atlas of human subcortical brain nuclei. *Sci Data* **5**, 180063 (2018). https://doi.org/10.1038/sdata.2018.63

90 Friston, K. J. *et al.* Bayesian model reduction and empirical Bayes for group (DCM) studies. *Neuroimage* **128**, 413-431 (2016). https://doi.org/10.1016/j.neuroimage.2015.11.015

91 Zeidman, P. *et al.* A guide to group effective connectivity analysis, part 2: Second level analysis with PEB. *Neuroimage* **200**, 12-25 (2019). https://doi.org/10.1016/j.neuroimage.2019.06.032

92 Rosa, M. J., Friston, K. J. & Penny, W. Post-hoc selection of dynamic causal models. *J Neurosci Meth* **208**, 66-78 (2012). https://doi.org/10.1016/j.jneumeth.2012.04.013

93 Edlow, B. L. *et al.* 7 Tesla MRI of the ex vivo human brain at 100 micron resolution. *Scientific data* **6**, 244 (2019).

Table 1.

Comparison of Characteristics Between Healthy Controls and Clinical Participants

	Healthy Controls (*N* = 77)		Clinical Participants (*N* = 70)			
Characteristics	Mean or N	*SD* or Percentage	Mean or N	*SD* or Percentage	Effect size (φ, Δ, or *d*)	*p*
Age (years)	22.78	4.1	22.29	5.3	.10	.264
Female	43	55.8	51	72.9	.28	.003
Education years)	13.8	1.3	13.5	1.2	.21	.098
DASS Total	7.62	6.0	27.16	11.2	-1.74	<.001
DASS Depression	2.40	2.2	10.14	5.5	-1.78	<.001
DASS Anxiety	1.78	1.9	7.06	4.2	-1.26	<.001
Depressive Disorder	-	-	41	58.6	-	-
MDD	-	-	29	41.4	-	-
PDD	-	-	12	17.1		
Anxiety Disorder	-	-	36	51.4	-	-
GAD	-	-	25	35.7	-	-
SAD	-	-	16	22.9	-	-
Specific Phobia	-	-	4	5.7	-	-
Panic Disorder	-	-	2	2.9	-	-
Stress Disorders			13	18.8		
PTSD	-	-	10	14.3	-	-

Adjustment Disorder	-	-	3	4.3		
Eating Disorders	-	-	7	10		
BED	-	-	3	4.3		
AN	-	-	2	2.9		
BN	-	-	2	2.9		
Antidepressant Use	-	-	14	19.7	-	-

Abbreviations: Anorexia Nervosa (AN); Binge-eating Disorder (BED); Bulimia Nervosa (BN); Depression Anxiety Stress Scale (DASS); Generalized Anxiety Disorder (GAD); Major Depressive Disorder (MDD); Persistent Depressive Disorder (PDD); Post-traumatic Stress Disorder (PTSD); Social Anxiety Disorder (SAD).

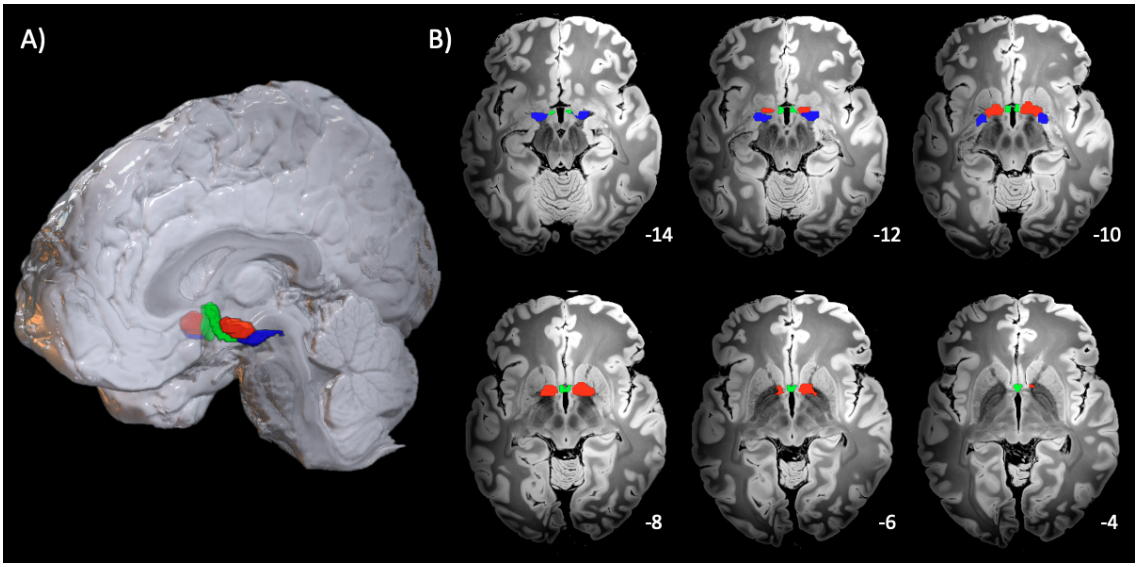

Figure 1. Basal forebrain masks used in the effective connectivity analysis. A) Render and B) axial slices of the Ch1-3 (green), Ch4 (blue), and VP (red) masks on the "Synthesized_FLASH25" (500 μm, MNI space) ex vivo template [93].

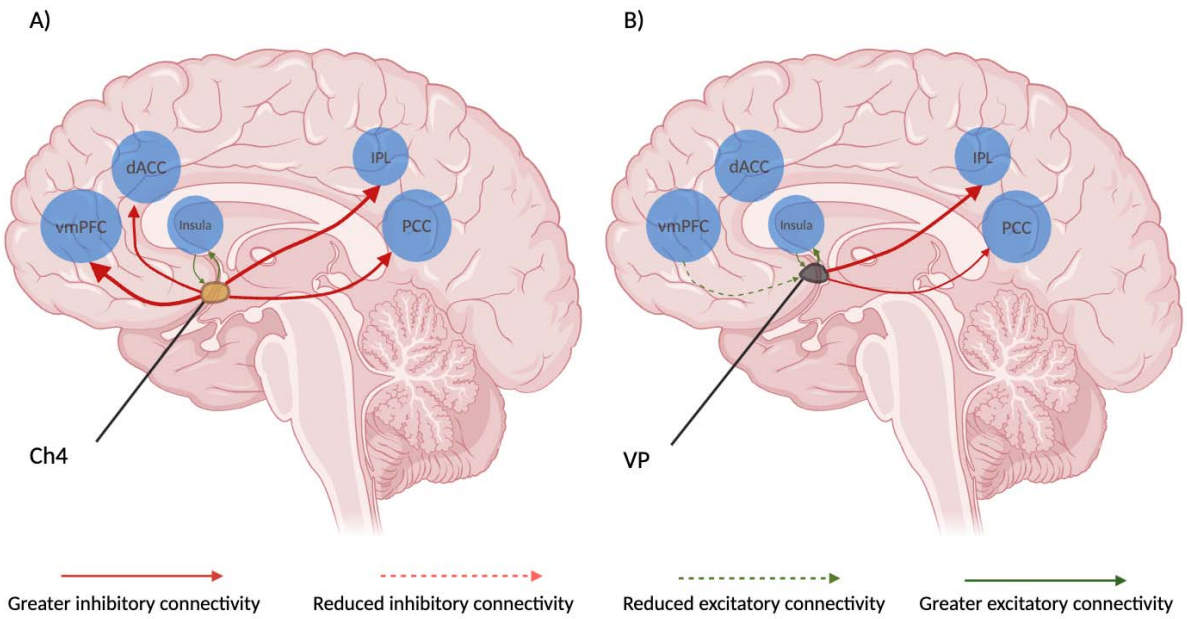

Figure 2. Differences in effective connectivity from the basal forebrain to cortical brain regions in clinical participants compared with healthy controls. Results indicate effects involving A) Ch4 (yellow) and B) ventral pallidum (black). Arrows have been weighted to indicate the relative size of the effects. Image created with BioRender (www.biorender.com).

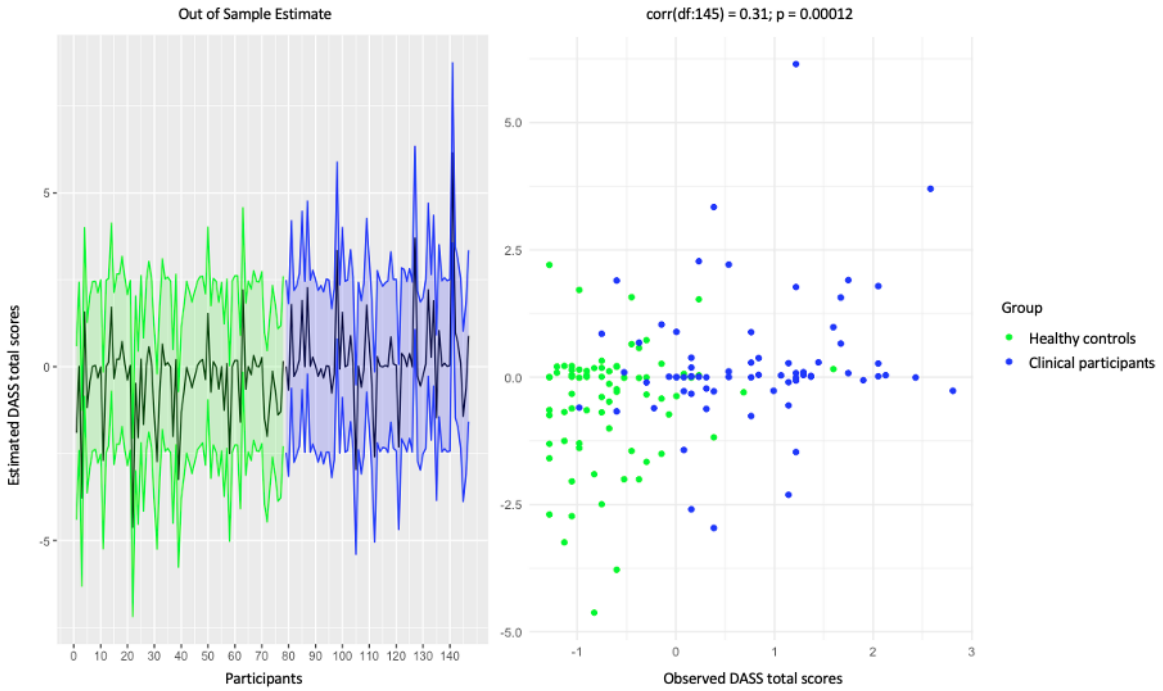

Figure 3. Leave-one-out cross-validation predicting DASS total scores for each participant. **Left:** The out-of-samples estimated of the DASS total score (z-scored) with 90% credible interval (shaded area). **Right:** The correlation between observed scores and the expected values for each individual participant using altered connections. Healthy controls are shown in green, clinical participants are shown in blue.